pharmaceuticals

MDPI

Article

Expanding the Structural Diversity of DNA Methyltransferase Inhibitors

K. Eurídice Juárez-Mercado [1], Fernando D. Prieto-Martínez [1], Norberto Sánchez-Cruz [1], Andrea Peña-Castillo [1], Diego Prada-Gracia [2] and José L. Medina-Franco [1,*]

[1] DIFACQUIM Research Group, Department of Pharmacy, School of Chemistry, National Autonomous University of Mexico, Avenida Universidad 3000, Mexico City 04510, Mexico; kaeuridice@gmail.com (K.E.J.-M.); ferdpm4@hotmail.com (F.D.P.-M.); norberto.sc90@gmail.com (N.S.-C.); andrea.pecas93@gmail.com (A.P.-C.)

[2] Research Unit on Computational Biology and Drug Design, Children's Hospital of Mexico Federico Gomez, Mexico City 06720, Mexico; prada.gracia@gmail.com

* Correspondence: medinajl@unam.mx

Abstract: Inhibitors of DNA methyltransferases (DNMTs) are attractive compounds for epigenetic drug discovery. They are also chemical tools to understand the biochemistry of epigenetic processes. Herein, we report five distinct inhibitors of DNMT1 characterized in enzymatic inhibition assays that did not show activity with DNMT3B. It was concluded that the dietary component theaflavin is an inhibitor of DNMT1. Two additional novel inhibitors of DNMT1 are the approved drugs glyburide and panobinostat. The DNMT1 enzymatic inhibitory activity of panobinostat, a known pan inhibitor of histone deacetylases, agrees with experimental reports of its ability to reduce DNMT1 activity in liver cancer cell lines. Molecular docking of the active compounds with DNMT1, and re-scoring with the recently developed extended connectivity interaction features approach, led to an excellent agreement between the experimental IC_{50} values and docking scores.

Keywords: dietary component; epigenetics; enzyme inhibition; focused library; epi-informatics; multitarget epigenetic agent; natural products; chemoinformatics

Citation: Juárez-Mercado, K.E.; Prieto-Martínez, F.D.; Sánchez-Cruz, N.; Peña-Castillo, A.; Prada-Gracia, D.; Medina-Franco, J.L. Expanding the Structural Diversity of DNA Methyltransferase Inhibitors. *Pharmaceuticals* **2021**, *14*, 17. http://dx.doi.org/10.3390/ph14010017

Received: 20 November 2020
Accepted: 23 December 2020
Published: 27 December 2020

1. Introduction

Historically, the term "epigenetics" is rooted in Waddington and Nanney's work, where it was initially defined to denote a cellular memory, persistent homeostasis in the absence of an original perturbation, or an effect on cell fate not attributable to changes in DNA [1,2]. However, "epigenetics" is now used with multiple meanings, for instance, to describe the heritable phenotype (cellular memory) without modification of DNA sequences [3], or the mechanism in which the environment conveys its influence to the cell, tissue, or organism [4]. Regardless of the different definitions, the interest in epigenetic drug discovery has increased, as revealed by the multiple approved epigenetic drugs or compounds in clinical development for epigenetic targets [5,6].

DNA methyltransferases (DNMTs) are one of the primary epigenetic modifiers. This enzyme family is responsible for promoting the covalent addition of a methyl group from *S*-adenosyl-*L*-methionine (SAM) to the 5-carbon of cytosine, mainly within CpG dinucleotides, yielding *S*-adenosyl-*L*-homocysteine (SAH) [7]. DNMT1, DNMT3A, and DNMT3B participate in DNA methylation in mammals to regulate embryo development, cell differentiation, gene transcription, and other normal biological functions. Abnormal functions of DNMTs are associated with tumorigenesis and other diseases [7,8].

DNMTs were the first epigenetic targets for which inhibitors received the approval of the Food and Drug Administration (FDA) of the USA: the nucleoside analogs 5-azacitidine (Vidaza) and decitabine or 5-aza-2′-deoxycytidine (Dacogen) (Figure 1), approved in 2004 and 2006, respectively, for the treatment of the myelodysplastic syndrome [9]. DNMTs

are promising epigenetic targets for the treatment of several types of cancer, including acute myeloid leukemia and colorectal, pancreatic, lung, ovarian, and breast cancer, which have been reviewed comprehensively [8,10]. Furthermore, DNMTs are also attractive targets for the investigation or treatment of other diseases such as diabetes [11], as well as autoimmune [12] and neurological disorders [13]. Inhibitors of DNMTs are also emerging as programs to develop combination therapies in drug cocktails or compounds targeting more than one epigenetic target simultaneously [14]. For instance, Rabal et al. recently reported dual inhibitors of DNMT1 and G9a histone methyltransferase [15,16]. Yuan et al. described a dual DNMT and histone deacetylase inhibitor (HDAC) inhibitor [17]. Hydralazine is an antihypertensive drug and a weak inhibitor of DNMT1 (Figure 1) [18]. This compound has been proved in several cancer cell lines, and there are studies that demonstrated that it is an inhibitor of DNMT1 with an IC_{50} of 2 μM for A549 cell line (human lung cancer cell line harboring wild-type p53), an IC_{50} of 20 μM for U373MG cell line (human glioblastoma cell line harboring inactive mutant p53) [19], and an IC_{50} of 30 μM for Hut78 cell line (cutaneous T cell lymphoma) [20,21].

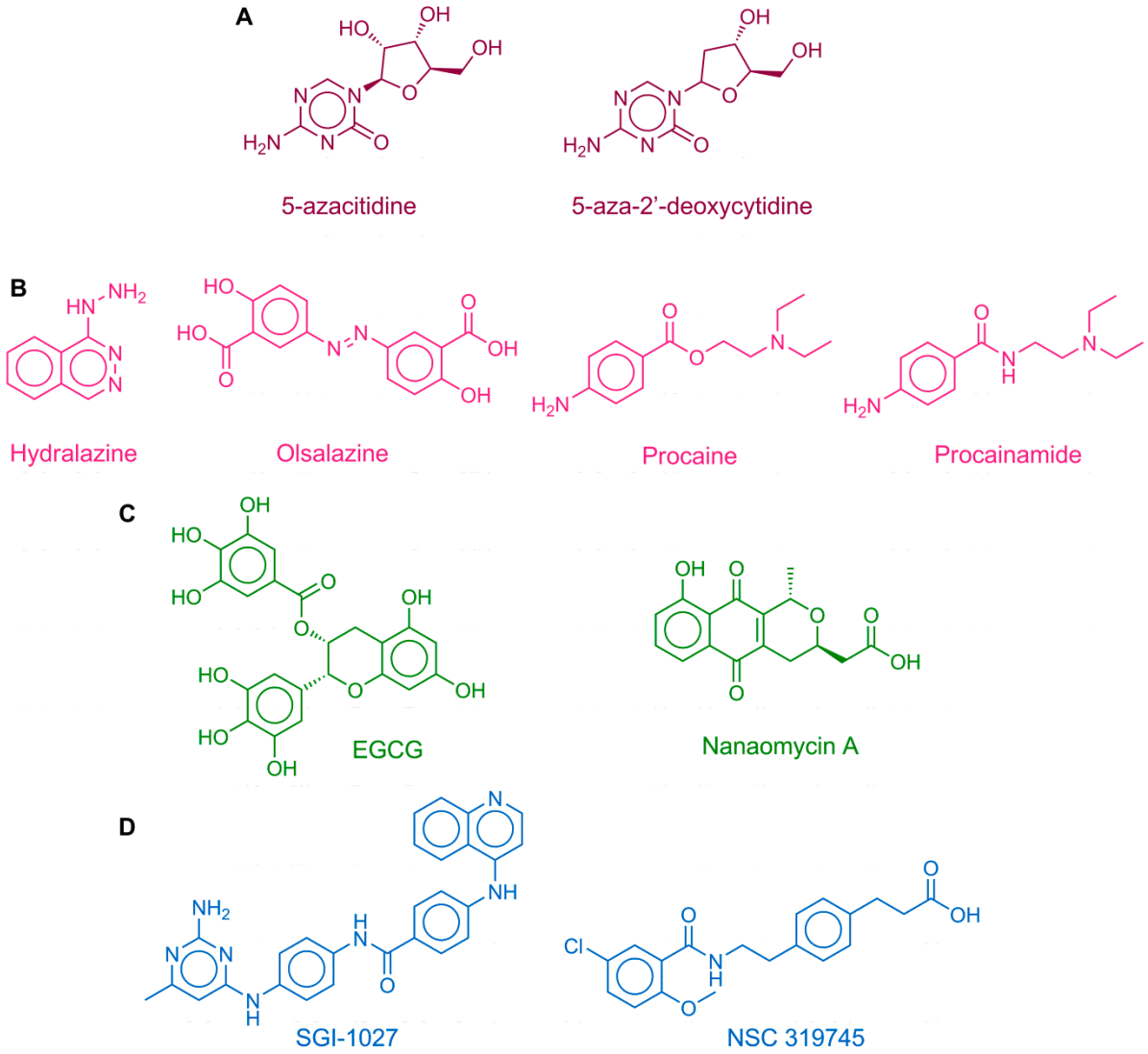

Figure 1. Chemical structures of representative DNA methyltransferase (DNMT) inhibitors and other compounds with associated hypomethylating properties from different sources. (**A**) approved drugs; (**B**) drug repurposing; (**C**) natural products and dietary components; (**D**) small molecules: synthetic compounds.

Despite the fact there are two DNMT inhibitors approved for clinical use, both azacitidine and decitabine have low specificity, poor bioavailability, and instability in physiological conditions and toxicity. Therefore, it has been the interest of our [22–29] and several other research groups [30–37] to identify DNMT inhibitors with novel chemical scaffolds for further development. Inhibition of DNMTs remains a major topic of research not only because of its potential therapeutic benefits but also to understand the essential mechanisms of epigenetic events in cells. There are currently more than 256 compounds in annotated public chemical databases [38] with measured activity vs. DNMTs. Figure S1 in the Supplementary Materials shows the most frequent scaffolds of active molecules. Figure 1 shows the chemical structures of representative DNMT inhibitors or compounds with DNA demethylation activity from different sources, including drugs for other indications, screening compounds from synthetic origin, and natural products [39–41]. Moreover, there are several compounds from dietary origin [42–44]. Of note, strong evidence indicates that environmental factors and nutrients play a major role in establishing epigenetic mechanisms, including irregular DNA methylation patterns. Thus, a regular uptake of DNA demethylating agents (which are not necessarily very potent DNMT inhibitors) is hypothesized to have a chemopreventive effect [45].

The DNMT inhibitors have been identified from different approaches or their combination [45,46] such as virtual screening [22,31], high-throughput screening, lead optimization [35,47], and structure-guided design [37], to name a few. Amongst the most promising inhibitors are molecules with "long scaffolds" such as the quinolone-based **SGI-1027** (Figure 1) and analogs. With the aid of molecular modeling, it has been hypothesized that such compounds with long scaffolds occupy the catalytic site and SAM's cavity [48]. It has also been proposed that analogs of **SGI-1027** exert their mechanism through interaction with DNA [49].

As part of an ongoing effort to identify novel DNMT1 inhibitors from different sources and further increase the availability of novel scaffolds, herein, we report five new inhibitors of DNMT1 with distinct chemical scaffolds. Two compounds, glyburide and Panobinostat, are approved drugs with potential drug-repurposing applications. In particular, panobinostat is a pan-histone deacetylase inhibitor (HDAC), another major epigenetic target, and could be used as a dual epigenetic agent.

2. Results

2.1. Biochemical DNMT Assays

Table 1 summarizes the relative enzymatic activities of DNMT1 and DNMT3B in the presence of 100 μM compound. Compounds that had more than 20% inhibition were regarded as inhibitors and were moved forward to dose–response evaluations. We used a similar criterion in a previous identification of novel chemical scaffolds [22]. Seven molecules showed detectable inhibition with DNMT1, of which the five most active were theaflavin (65% inhibition), **CSC027694519** (65%), panobinostat (63%), **7936171** (62%), and glyburide (60%). The least active were **CSC027480404** (29%) and **CSC026286840** (27% inhibition). Theaflavin and **7936171** showed detectable inhibition with DNMT3B (33 and 22% inhibition, respectively). All other eight molecules were inactive with DNMT3B.

The five compounds with the highest percentage of inhibition at 100 μM with DNMT1 were tested in a dose–response manner. Theaflavin that showed the best activity at a single dose with DNMT1 and DNMT3B was also tested in a dose–response manner with DNMT3B and DNMT3B/3L. Table 2 summarizes the results.

Table 1. Results of the relative enzymatic activity of DNMT1 and DNMT3B as percentages [a].

Set	Compound	DNMT1	DNMT3B
Approved drug	Glyburide	40.04 (±0.78)	95.97 (±4.76)
Approved drug	Panobinostat	37.31 (±1.80)	103.05 (±0.59)
Dietary component	Theaflavin	34.62 (±0.06)	66.75 (±1.11)
Inhibitor of the viral NS5 RNA methyltransferase	**7936171**	37.74 (±2.15)	78.20 (±0.30)
DNMT-focused library	**CSC027480404**	70.63 (±0.19)	96.39 (±0.28)
DNMT-focused library	**CSC026286840**	73.45 (±3.06)	90.59 (±2.49)
DNMT-focused library	**CSC027694519**	35.42 (±1.78)	97.42 (±2.49)
DNMT-focused library	**6631802**	93.26 (±7.97)	93.54 (±0.54)
DNMT-focused library	**CSC027796832**	107.25 (±0.59)	95.28 (±0.47)
DNMT-focused library	**CSC027083851**	105.71 (±1.27)	97.85 (±5.66)

[a] Mean value of two measurements ± standard deviation. Compounds with an inhibition greater than 20% are marked in blue.

Table 2. Results of dose–response evaluations for selected compounds (IC_{50}) with DNMT1 [a].

Set	Compound	DNMT1 (IC_{50} μM)
Approved drug	Glyburide	55.85 (±1.11)
Approved drug	Panobinostat	76.78 (±0.23)
Dietary component	Theaflavin [b]	85.33 (±0.14)
Inhibitor of the viral NS5 RNA methyltransferase	**7936171**	78.53 (±8.60)
DNMT-focused library	**CSC027694519**	85.11 (±4.10)

[a] Mean value of two measurements. SAH was included as a positive control (IC_{50} of 0.26 μM); [b] also evaluated with DNMT3B and DNMT3B/3L. The IC_{50} was > 100 μM.

The two approved drugs, glyburide and panobinostat, inhibited DNMT1 with IC_{50} values of 55.85 and 76.78 μM, respectively. Theaflavin had an IC_{50} value of 85.33 μM. The other two small molecules **793617** and **CSC027694519** had IC_{50} values of 78.53 and 85.1 μM, respectively. SAH was used as a non-specific positive control and confirmed its effective inhibition of DNMT1 with an IC_{50} of 0.26 μM under the assay's conditions. Theaflavin, which showed the best activity at a single dose with DNMT1 and DNMT3B (Table 1), was also tested in a dose–response manner with DNMT3B and DNMT3B/3L showing, in both cases, IC_{50} values > 100 μM.

2.2. Molecular Docking and Re-Scoring

The docking was performed in Molecular Operating Environment (MOE) v.2018 for the 10 compounds (shown in Figure 2) in the active site of the crystal structure of the catalytic domain of DNMT1 (PDB ID: 4WXX), as described in the Materials and Methods section. The docking scores ranged from −8.35 to −7.09 kcal/mol. The scores for the five compounds tested in the biochemical assays in dose–response evaluations ranged from −8.20 to −7.42 kcal/mol. Table 3 summarizes the results of docking with MOE and re-scoring with extended connectivity interaction features (ECIF) (see the Materials and Methods section).

Figure 3 shows the 2D interaction maps of the predicted binding mode between the human catalytic domain of DNMT1 and the five compounds evaluated in a dose–response manner: glyburide, panobinostat, theaflavin, **793617**, and **CSC027694519.** These interactions correspond to the docking poses with the most favorable docking scores, as calculated with MOE. All the compounds had predicted interactions with catalytic residues and showed hydrogen bond interactions with Glu 1266. Furthermore, glyburide, panobinostat, theaflavin, and **CSC027694519** also showed π–H interactions.

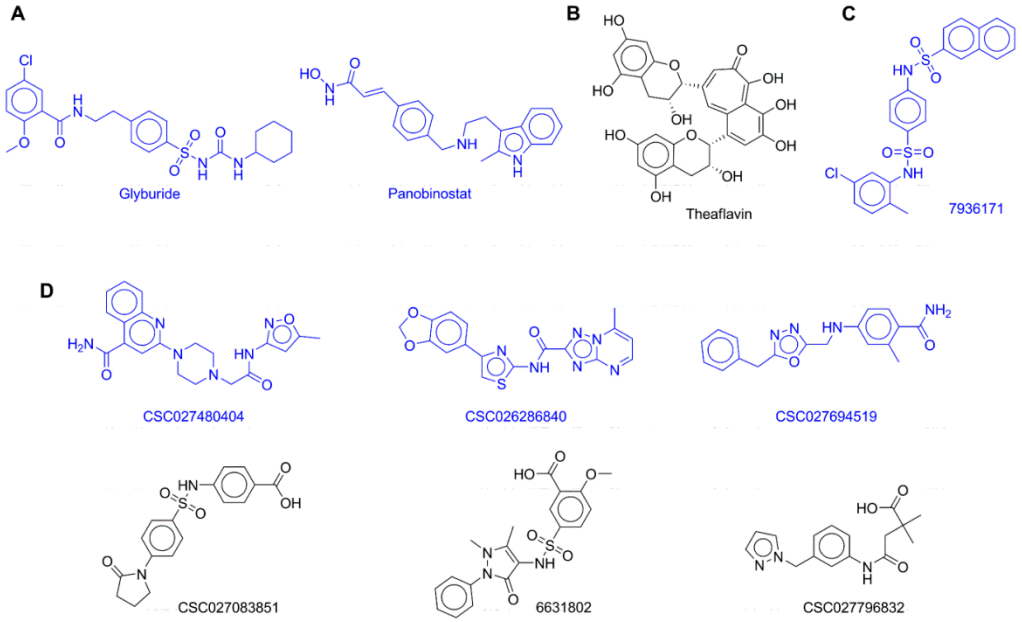

Figure 2. Chemical structures of 10 compounds from different sources experimentally tested. Compounds are grouped by their source: (**A**) approved drugs; (**B**) dietary source (natural product); (**C**) inhibitor of the viral NS5 RNA methyltransferase; (**D**) DNMT-focused library.

Table 3. Summary results of docking with Molecular Operating Environment (MOE) and re-scoring with extended connectivity interaction features (ECIF).

ID	ECIF Score [a]	MOE Score	pIC_{50}	% Inhibition
Glyburide	7.38	−8.20	4.25	59.96
Panobinostat	6.36	−7.34	4.11	62.69
Theaflavin	6.48	−8.16	4.07	65.38
7936171	6.52	−7.67	4.11	62.26
CSC027694519	5.85	−7.71	4.07	64.58
6631802	7.26	−8.35	ND [b]	6.74
CSC027796832	5.50	−7.09	ND	−7.25
CSC027480404	6.62	−8.15	ND	29.97
CSC026286840	6.69	−8.28	ND	26.55
CSC027083851	6.81	−7.42	ND	−5.71
SAH	5.25	−9.48	6.59	ND

[a] Predictions from ECIF6::LD-GBT; [b] ND: not determined.

The docking poses of the five compounds were re-scored with ECIF, as described in the Materials and Methods section. Table 3 summarizes the results of the predictions from ECIF6::LD-GBT for the docking poses generated with MOE. For the five compounds tested in a dose–response manner, the table shows the results of the IC_{50} as the -log value (pIC_{50}). The table indicates that among the five compounds with pIC_{50} values, the most active, glyburide, was predicted correctly by the ECIF re-scoring method. Moreover, the re-scoring of MOE poses ranked glyburide as the one with the highest affinity overall, while MOE score predicted a higher affinity for compounds **6631802** and **CSC026286840**. Figure 4 shows the association between the experimental pIC_{50} of the five compounds evaluated in biochemical inhibition assays of DNMT1 with the MOE's docking scores (Figure 4A) and re-scoring with ECIF6::LD-GBT (Figure 4B). Clearly, the ECIF re-scoring scheme improved the correlation with the experimental pIC_{50} values.

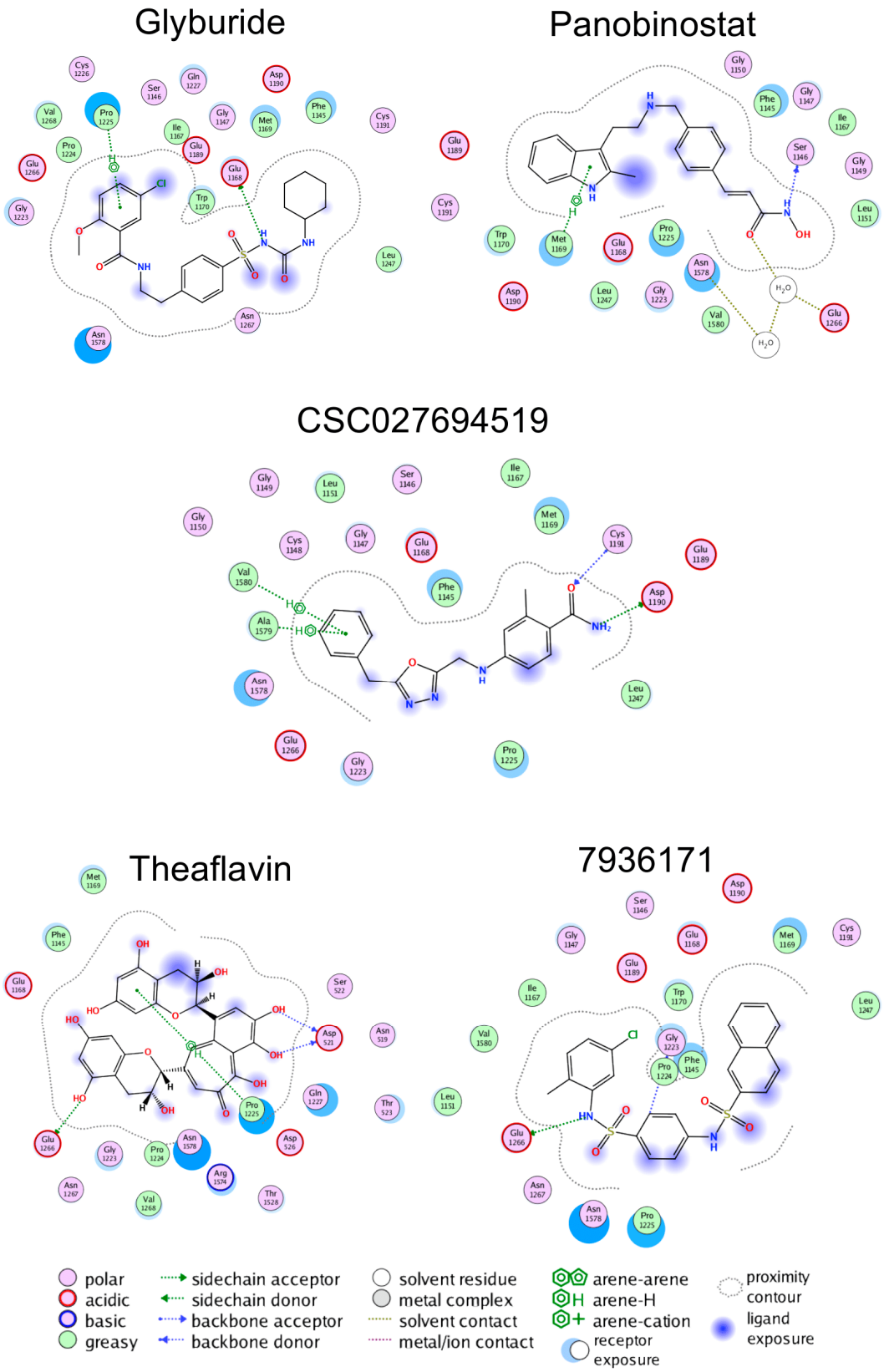

Figure 3. Binding poses predicted with the Molecular with Molecular Operating Environment v.2018 of the five active compounds with the catalytic domain of DNA methyltransferase 1.

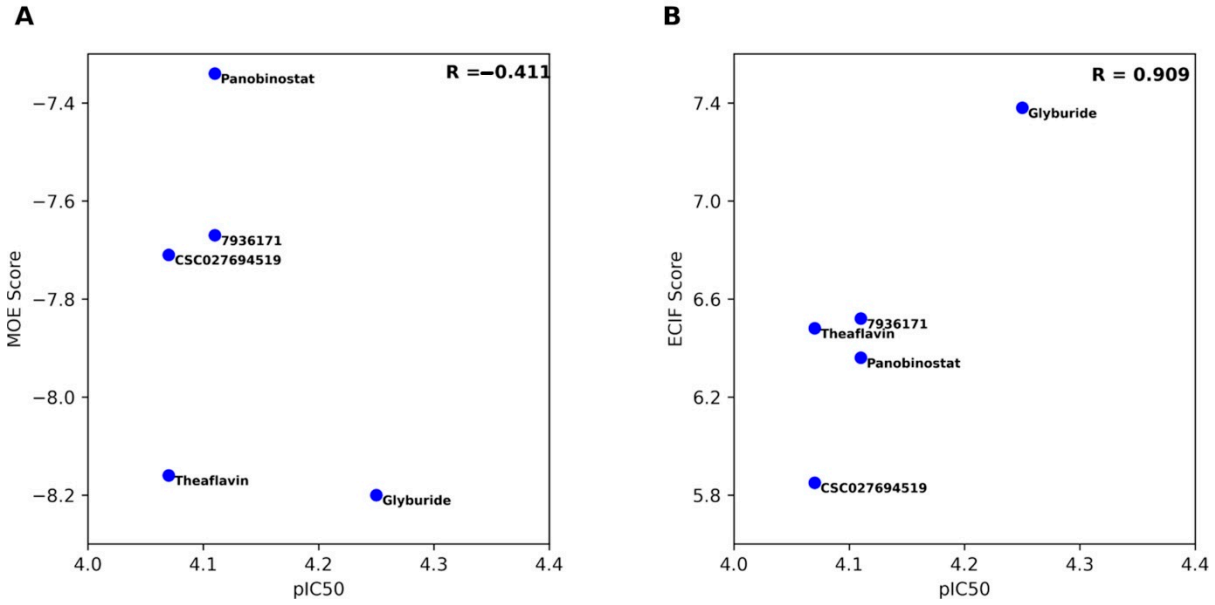

Figure 4. Correlation between the experimental pIC_{50} of the five compounds evaluated in biochemical inhibition assays of DNMT1 with (**A**) the docking scores calculated with MOE, and (**B**) the ECIF6::LD-GBT scores.

2.3. Molecular Dynamics and Adaptive Sampling

Molecular dynamics (MD) simulations were conducted to determine the putative binding mode and interactions of glyburide and DNMT1. To this end, six docking poses (Figure S3 in the Supplementary Materials) were selected as the starting points of the MD simulations in question. With these, kinetic transition networks (KTNs) were constructed to determine microstates (on the basis of protein–ligand contacts obtained with YASARA) and their associated probability. Only the trajectory from "**pose 6**" showed a microstate network (Figure S4 in the Supplementary Materials) with higher probability than other poses (data not shown). To confirm this observation, we conducted "random walks" using implicit solvation, as this often favors faster transitions [50].

Simulation data were postprocessed with PyEMMA, using different features for microstate definition and construction of preliminary Markov state models (MSMs). At this stage, only inverse distances between the carbonyl atoms of glyburide and DNMT1 (Cα atoms) showed metastability by means of time-lagged independent component analysis (TICA) and k-means clustering (Figure 5A). Using spectral analysis along eigenvalues with the Robust Perron Cluster Analysis (PCCA+) [51], we determined microstate density and distribution (Figure 5B); finally, contact frequency along these samples was calculated for comparison (Figure 5C).

Microstate distributions showed that glyburide favored hydrophobic contacts within the SAH binding site, with transitions between hydrogen bonding and hydrophobic contacts for Phe1145, Trp1170, and Asn1578. On the basis of these observations, we decided to conduct end-point calculations by means of molecular mechanics/Poisson-Boltzmann Surface Area (MM/PBSA) using **pose 6** trajectory (in explicit solvent), yielding a ΔG value of -48.7 ± 4.6 kcal/mol.

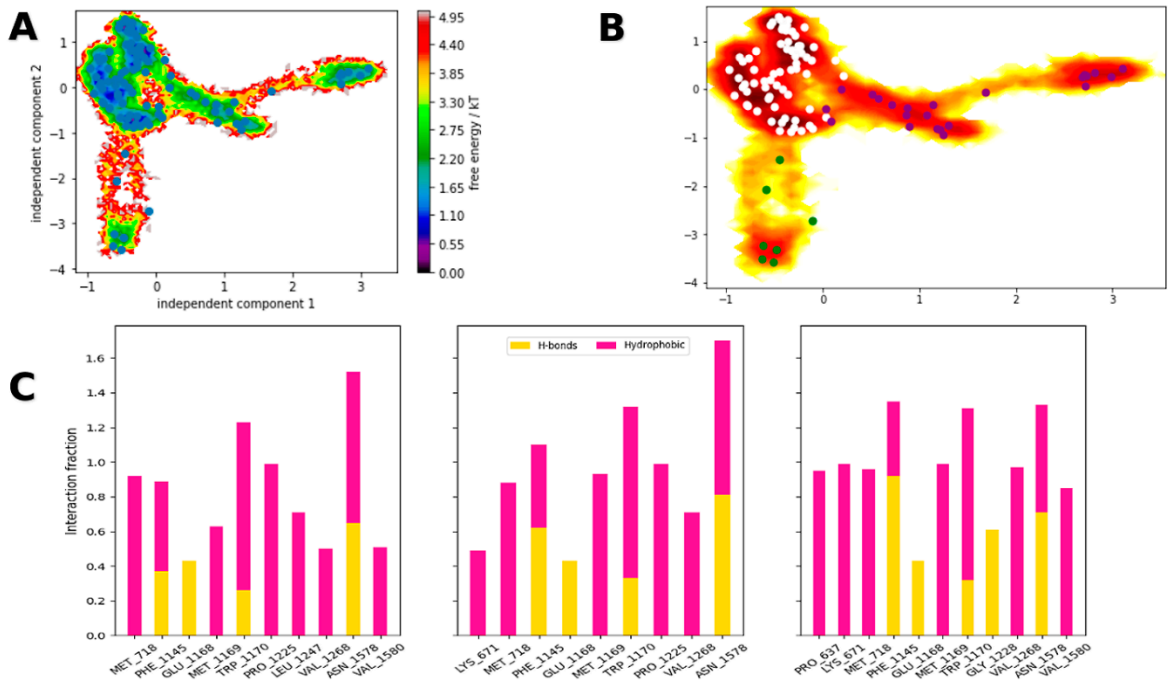

Figure 5. Free energy landscape of the glyburide–DNMT1 complex along the slowest independent components (**A**); microstate distribution as obtained with the Perron Cluster Analysis PCCA+ sampling (**B**); contact frequency obtained from the discretized microstates (**C**).

3. Discussion

3.1. Biochemical DNMT Assays

The initial goal of this study was to identify novel small molecule DNMT1 and DNMT3B inhibitors. In this work, we deprioritized testing with DNMT3A because it has been reported that this enzyme can act as both an oncogene and as a tumor suppressor gene, at least in lung cancer (it remains to be tested as to whether this paradox of DNMT3A applies to other cancers) [8]. Seven molecules with detectable inhibition of DNMT1 and two with DNMT3B were initially identified at single dose concentrations (Table 1). An approved drug for the treatment of type 2 diabetes (glyburide) and an approved anticancer drug known as HDAC inhibitor (panobinostat) were among the active compounds with DNMT1. Other active compounds against DNMT1 were a dietary component (theaflavin), a naphthalene sulfonamide (**7936171**) previously reported to be an inhibitor of dengue virus methyltransferase [52], and three small molecules from a DNMT focused library (**CSC027480404**, **CSC026286840**, and **CSC027694519**).

Overall, the tested compounds showed less activity with DNMT3B (Table 1). Only two compounds, the dietary component theaflavin, and the naphthalene sulfonamide, showed inhibition higher than 20% with DNMT3B at high concentration. Moreover, theaflavin showed the highest percentage of inhibition (33%), which was lower than the highest percentage of inhibition showed for DNMT1 (65%). None of the two compounds had an IC_{50} lower than 100 μM with DNMT3B.

Dose–response assays for the most active compounds at a single dose (Table 2) revealed that, under the assay conditions used in this study, the two approved drugs glyburide and panobinostat had the lowest IC_{50} values (55.85 and 76.78 μM, respectively). The other three active compounds (**7936171**, theaflavin, and **CSC027694519**) had IC_{50} values between 78.5 and 85 μM. Overall, these IC_{50} values were relatively high. However, it should be noted that standard biochemical assays for DNMT enzymes have not been fully established and the results show a large variation between assay conditions. This point has been largely discussed in the literature for DNMT inhibitors [48,53]. In this work, we used SAH as a

positive control, since SAH is a very well known inhibitor of DNMT [54]. Even though the active compounds' potency values are not high, all compounds have chemical scaffolds different from the scaffolds reported for known DNMT inhibitors.

Glyburide (Figure 2) is a sulfonylurea. In 1984, it received approval by the United States FDA for the treatment of patients with diabetes mellitus type II. To the best of our knowledge, there are no reports of this compound as an inhibitor of DNMT1. However, several studies support that sulfonylureas are potential anticancer drug candidates for several cell lines such as colon cancer, human ovarian cancer, kidney cancer, melanoma, and lung cancer [55,56]. Therefore, we propose that glyburide could be further investigated and developed as an epi-drug with potential anticancer activity.

Panobinostat is an orally available pan-deacetylase inhibitor with broad antitumor activity [57]. It has shown inhibitory activity vs. different types of cancer, for example, malignant glioma cells with an IC_{50} range of 0.3 μM to 0.23 μM [58], carcinoma cells (IC_{50} between 0.4 nM and 1.3 nM) [59], and in human erythroleukemic cell lines (IC_{50} between 40 nM and 51 nM) [60]. One of the principal benefits of the panobinostat is that being an HDAC inhibitor will avoid the histone acetylation, which helps to maintain that the chromatin is closed and decrease the gene transcription involved with proliferation, differentiation, and progress of the cancer cells. Zopf et al. reported that panobinostat reduced DNMT1 (and DNMT3a) activities and expression in liver cancer cell lines [61]. In the study of Zopf et al., the authors concluded that inhibitors of HDACs can indirectly control DNA methylation. In this work, it was confirmed that panobinostat also inhibits the enzymatic activity of DNMT1 directly. Of note, there is a recent interest in developing dual inhibitors of DNMTs and HDACs, and results in this direction appear promising [17]. Indeed, Yuan et al. reported hydroxamic acid derivatives of a small molecule previously identified as a weak inhibitor of DNMT1 from virtual screening of a large chemical library [22]. In the work of Yuan et al., the hydroxamic acid derivatives of NSC 319745 showed inhibition of DNMT1, HDAC1, and HDAC6, plus cytotoxicity activity against human cancer cells [47]. In a second example in the clinic, the combined use of decitabine (a DNMT inhibitor) and belinostat (an HDAC inhibitor) increased the chemotherapy efficiency [62]. Moreover, Min et al. showed that an increase in transcription of DNMT1 is one of the mechanisms of resistance of anti-cancer drugs targeting HDACs, such as vorinostat. Consequently, it has been shown that co-targeting DNMT1 improved the antitumor efficacy of vorinostat and other HDAC inhibitors [63]. These contributions, including the findings of this work, are in line with the epigenetic multitargeting. The advantages of this approach have been demonstrated in both in vitro and in vivo disease models by the co-administration of an epigenetic agent with another drug [64].

The naphthalene sulfonamide **7936171** (also with ID ZINC 01078518) is a known inhibitor of the viral NS5 RNA methyltransferase with an IC_{50} of 64.2 μM and an EC_{50} of 12 μM [52]. The viral RNA domain involves the use of SAM as the methyl donor and generates SAH as the final product. Compound **7936171** has a "long" and different scaffold from the known DNMT1 inhibitors published thus far (Figure S1).

Theaflavin is a natural product polyphenol found in green and black tea and coffee (vide supra) with previously measured enzymatic inhibitory activity of DNMT3A [65]. However, there were no reports on its inhibitory potential of DNMT1 and DNMT3B. In this work, we measured for the first time its activity with both enzymes. Despite the fact its IC_{50} is high (85.3 μM, under the assay conditions of this work), this dietary component could contribute to the modulation of DNMT1. Interestingly, it has been proposed that the modulation of normal levels of DNMT could be conveniently achieved through the dietary uptake of food chemicals (or other "safe" natural products). A prominent example of this hypothesis has been suggested for the polyphenol compound from green tea, EGCG (Figure 1), which has been proposed to inhibit DNMT1 and reactivate methylation-silenced genes in cancer [45].

The other two small molecules, **7936171** and **CSC027694519**, had no previous reports of inhibition of DNMTs. As discussed in the next section, both molecules have drug-

like characteristics and have novel scaffolds that can be further optimized for DNMT1 inhibition.

3.2. Computational Studies

Herein, we employed in silico methods to rationalize at the molecular level the experimental results of the most active molecules. Of the different mechanisms described to inactivate DNMT activity [66], we hypothesized that the herein identified inhibitors are SAM competitors. This hypothesis is based on the "long" scaffolds of the active compounds such as glyburide, panobinostat, **7936171**, and **CSC027694519**. The predicted binding modes suggested strategies for the structure-based optimization of the small molecules. For instance, comparing the predicted binding mode of **CSC027694519** with the co-crystallized position of SAH in PDB ID: 4WXX (Figure S2 in the Supplementary Materials) suggests that substitution with a polar group in the benzyl ring of **CSC027694519** could enhance the affinity, making polar or hydrogen bond contacts with amino acid residues such as Ser1146, Gly1150, Leu1151, and Val1580 (by comparison with the primary amine or carboxylate groups of SAH). Of note, **CSC027694519** already makes hydrogen bond interactions with the polar side chains of Asp1190 and Cys1191 (similar to the hydrogen bond contacts of SAH, Figure S2). Similarly, comparing the predicted binding mode of **7936171** with the co-crystallized position of SAH (Figure S2) suggests that the naphthalene ring of **7936171** could be replaced with polar heteroaromatic rings. Of course, the synthesis and testing of the analogs should be made, which is one of the major perspectives of this work. It remains to confirm the hypothesis of the putative binding site of these molecules that can be further tested experimentally with binding completion assays once more potent compounds are identified.

To gain some rationale behind the observed pIC_{50} of glyburide, we conducted molecular simulations to probe its putative binding mode in DNMT1. Using KTN models, we determined that **pose 6** had a higher contact stability. This pose had the urea moiety as the main anchor towards Glu1168, the main contact for charged amines, as described in previous works [67]. However, by means of adaptive sampling and Markov state models, we determined that three microstate distributions are possible for this binding mode. In these, a high prevalence of hydrophobic contacts with Met718, Trp1170, and Val1268 was observed. Moreover, a mixture of polar and hydrophobic interactions towards Phe1145, Trp1170, and Asn1578 was determined, with the latter showing the most concurrent profile along microstates, suggesting it as the presumptive anchor for glyburide. Hence, optimization around this scaffold could provide venues for ligand design without the need of charged groups.

On the basis of the Chapman–Kolmogorov test [68], researchers can only apply this preliminary model to small timescales. Thus, a more extensive validation is necessary to achieve a robust kinetic description of the possible binding/unbinding paths of glyburide; nonetheless, this goes beyond the current scope of this work. Furthermore, on the basis of ΔG values obtained from end-point calculations, we observed a better correlation with the experimental value, considering that similar predictions have been observed on other epi-modulators with IC_{50} values in the micromolar range [69]. This gives further support to the proposed binding mode and the experimental potency of glyburide.

4. Materials and Methods

We aimed to test compounds from different sources: approved drugs, synthetic compounds from a DNMT-focused library, and 1 compound from dietary origin. We experimentally tested 10 molecules with diverse chemical scaffolds and chemical structures different from reported DNMT inhibitors (Figure 2). Thus, we screened the following 2 approved drugs with "long" chemical scaffolds in biochemical assays as inhibitors of DNMTs (Figure 2A): the sulfonylurea glybenclamide, approved for the treatment of diabetes (vide infra), and panobinostat, a non-selective and potent zinc-dependent HDAC inhibitor (the most potent deacetylase inhibitor on the market), approved in 2018 by the FDA for the treatment

of multiple myeloma. Of note, currently epigenetic multitargeting is focused on the inhibition of zinc-dependent HDACs as one of the action mechanisms [14]. Due to the known activity of polyphenols and previous evidence of theaflavin activity with DNMT3A [65], we hypothesized that theaflavin, a dietary component (Figure 2B) present in black tea, is an inhibitor of DNMT1 and DNMT3B. We also theorized that the naphthalene sulfonamide **7936171** (Figure 2C) with a long scaffold is an inhibitor of DNMT1 and DNMT3B [52]. Finally, we tested six molecules from a DNMT-focused library of synthetic molecules (Figure 2D), which are becoming attractive to experimentally screen molecules [6]. To select the 10 compounds in this work, we used commercial availability and reasonable price (the latter an important factor considering the current economic situation imposed by the coronavirus disease 2019 (COVID-19) pandemic) as additional criteria.

First, the 10 compounds were tested at a single concentration (100 μM) in duplicate in a biochemical DNMT assay. SAH was used as a reference. The five most active molecules at one-single concentration were further tested in a dose–response manner to obtain the half-maximal inhibitory concentration (IC_{50}). Predicted binding modes for the five compounds were studied using molecular docking, implementing a novel re-scoring algorithm recently developed [70].

4.1. Compounds

All compounds were purchased from chemical vendors. Glyburide, panobinostat, and theaflavin were purchased from TargetMol. Molecules **7936171** and **6631802** were purchased from Chembridge Corporation. Molecules **CSC027480404**, **CSC026286840**, **CSC027694519**, and **CSC027083851** were acquired from ChemSpace. The compound purity confirmed by the chemical vendors was equal or higher than 90% (Table S1 in the Supplementary Materials).

4.2. Biochemical DNMT Assays

The inhibition of the enzymatic activity of DNMT1, DNMT3B, and DNMT3B/3L was tested using the HotSpot^{SM} platform for methyltransferase assays available at Reaction Biology Corporation [71]. HotSpot^{SM} is a low volume radioisotope-based assay that uses tritium-labeled AdoMet (^{3}H-SAM) as a methyl donor. The test compounds diluted in dimethyl sulfoxide were added using acoustic technology (Echo550, Labcyte) into enzyme/substrate mixture in the nano-liter range. The corresponding reactions were commenced by the addition of ^{3}H-SAM and incubated at 30°C. Total final methylations on the substrate (Poly dI-dC in DNMT1 assay, and Lambda DNA in DNMT3B; DNMT3B/3L assay) were identified by a filter binding method implemented in Reaction Biology. Data analysis was conducted with Graphed Prism software (La Jolla, CA, USA) for curve fits. Reactions were carried out at 1 μM of SAM. In all assays, SAH was used as a standard positive control. The 10 compounds were tested first with DNMT1 and DNMT3B at one 100 μM concentration in duplicate. The 5 most active compounds were tested in 10-dose IC_{50} (effective concentration to inhibit DNMT1 activity by 50%) with a threefold serial dilution starting at 100 μM. Theaflavin was also tested with DNMT3B and DNMT3B/L in 10-dose IC_{50} with threefold serial dilution starting at 100 μM. The authors have previously contracted the screening services of Reaction Biology Corporation to identify a novel inhibitor of DNMT1 [24].

4.3. Molecular Docking and Re-Scoring

The 5 compounds were tested in a dose–response manner, and that showed activity with DNMT1 (vide infra) were docked with this enzyme using the program Molecular Operating Environment (MOE), version 2018.08 [72]. The chemical structures of the 5 compounds were built with MOE. The docking was carried out with the crystal structure of the catalytic domain of DNMT1 obtained from the Protein Data Bank [73] (PDB ID: 4WXX [74]). This crystal structure is in complex with SAH and has a resolution of 2.62 Å. The structure of the protein was prepared with the "QuickPrep" tool of MOE v.2018 using

the parameters established by default, which helped us to remove the molecules of structural water and to add hydrogens atoms to the protein. In this process, the co-crystallized SAH was removed for the binding site to realize a direct docking. The docking was conducted using default parameters in MOE. Before docking the 5 newly tested compounds, we validated the docking protocol by re-docking the SAH obtaining a root mean square deviation of 1.3 angstroms (and a docking score of −8.96 kcal/mol).

Docking poses obtained with MOE were re-scored with the extended connectivity interactions features (ECIF) method. Briefly, ECIF is a recently reported set of descriptors to represent protein–ligand complexes. These descriptors are defined as a set of protein−ligand atom-type pair counts relying on a detailed description of the connectivity of the atoms involved. It has been shown that machine-learning scoring functions built on ECIF and gradient boosting trees consistently outperform the performance of scoring functions reported thus far regarding the obtention of binding scores in a linear correlation with experimental data, particularly when a distance cutoff criterion of 6 angstroms is used to derive the descriptors, and purely ligand-based descriptors are added (ECIF6::LD-GBT) [70]. From the poses obtained from MOE, the best-ranked one for each compound was prepared using X-Tool [75] and standardized using Standardizer, JChem 20.11.0, 2020, ChemAxon to perceive aromaticity in an interpretable way for the model. All poses were re-scored using the ECIF6::LD-GBT model [70].

4.4. Probing the Putative Binding Mode of Glyburide

To gain further insight on the presumptive interaction between glyburide and DNMT1, we conducted molecular dynamics (MD) simulations, mostly due to the observed pIC_{50}. To this end, the PDB ID: 3SWR was prepared with PDBfixer (v.1.6), completing missing atoms and residues. This structure was further optimized with YASARA2 forcefield (YASARA; v.20.8.1; [76]). Docking of glyburide was carried out using PLANTS (v.1.2; [77]) with a definition of the binding site in a sphere of 15 Å around the co-crystallized molecule of sinefungin. Twenty poses were obtained and analyzed choosing those with a similar arrangement to sinefungin or in its vicinity. The change of software at this stage was due to PLANTS performance on several benchmarks for binding mode prediction [78]). Protein–ligand complexes were parametrized with AMBERTools19, using the AMBER14 forcefield [79] for protein and GAFF2 for glyburide; the metal centers of DNMT1 were parametrized using the Cationic Dummy Atom model (CaDA; [80,81]). Initial structures were then buffered in an ortorhombic cell extended 1.4 nm beyond the protein in every direction, and all systems were simulated with explicit solvent using the TIP3P model. The systems were simulated using OpenMM (v.7.4.1; [82]), beginning with an energy minimization using steepest descent algorithm, with a convergence threshold of 10 kJ/mol/nm. This was followed by an equilibration of 1 ns, where all water molecules and hydrogen bonds were constrained; simulation timestep was set to 2 fs using the Langevin integrator. Selected poses were then simulated under NPT ensemble for 100 ns at 300 K and 1 atm of pressure using the Andersen thermostat and Monte Carlo Barostat. Trajectories were analyzed with MDTraj [83] and YASARA for protein–ligand contacts. Additionally, contact networks were constructed with Networkx [84] and analyzed using OpenKTN (in house library).

Adaptive Sampling and End-Point Calculations

With the aid of kinetic transition networks (KTN; [85]), we identified the most probable microstates along MD trajectories. We then followed this with a series of random walks starting from these conformations, using implicit solvent simulations. These were also carried out with OpenMM, using the Onufriev–Bashford–Case (OBC) model with GB^{OBCII} parameters [76]). The "walks" were also analyzed with MDtraj and OpenKTN to determine new starting conformations to improve sampling and transitions along microstates. These data were further analyzed with PyEMMA (v.2.5.7; [86]), accounting for a total simulation time of 1 μs. We used trajectory featurization [87] to determine slow components and

metastability by means of time-lagged independent component analysis (TICA). With this information, preliminary Markov state models (MSMs) were constructed to gain insight on the kinetics of the system [88]. Finally, we used this information to conduct end-point calculations using the MM/PBSA method as implemented on APBS [89]).

5. Conclusions

DNMTs are a fundamental class of epigenetic regulatory enzymes. In this work, we tested 10 compounds with novel scaffolds as inhibitors of DNMT1 and DNMT3B in biochemical assays. Seven compounds showed at least 20% inhibition of DNMT1 at 100 μM. Five molecules showed activity in dose–response inhibition assays with DNMT1 with IC_{50} between 55.8 and 85.3 μM. Although the molecules' overall potency was not high under this work's assay conditions, four compounds were found to have novel chemical scaffolds not previously described as inhibitors of DNMT1 in biochemical assays. Notably, glyburide, an approved drug for diabetes type II treatment, showed the best potency of the compounds tested in this study and can be further investigated in its role in epigenetic mechanisms. Moreover, glyburide could be pursued for drug repurposing applications. It was also concluded that panobinostat is an inhibitor of the enzymatic activity of DNMT1. Remarkably, panobinostat, an epigenetic drug for treating different types of cancer, has shown inhibition of DNMT1 in liver cancer cell lines [61]. Therefore, it is concluded that panobinostat, a known HDAC inhibitor, can be further investigated as a multitarget epigenetic agent. In this work, we also concluded that theaflavin, a natural dietary product, inhibits DNMT1 and does not show significant inhibition of DNMT3B. Therefore, this work also complements theaflavin's DNMT activity profile that had reported activity with DNMT3A [65]. It was also concluded that compounds **7936171** and **CSC027694519** and the two compounds that showed 30% inhibition of DNMT1 at 100 μM (**CSC027480404** and **CSC026286840**) can be starting points of optimization programs to improve their potency.

Molecular docking of the most active compounds helped propose binding modes with the catalytic binding site of DNM1. Although MOE scores predicted SAH as the most potent inhibitor, the novel ECIF re-scoring scheme ECIF6::LD-GBT improved significantly the correlation of the docking scores calculated with MOE with the experimental pIC_{50} values considering the rest of the compounds. Therefore, docking with MOE for compound selection and re-scoring with ECIF for prioritizing experimental tests can guide the optimization programs of the DNMT1 inhibitors identified in this work, which is one of the main perspectives of this work. Another perspective is testing the DNA demethylation activity of the most active compounds. This can be achieved directly with **7936171** and **CSC027694519** or after the compounds are optimized.

Supplementary Materials: The following are available online at https://www.mdpi.com/1424-8247/14/1/17/s1, Figure S1: Chemical structures of the 10 most frequent (Bemis–Murcko) scaffolds of the active DNMT inhibitors available in ChEMBL 27. Table S1: Chemical vendors of the 10 compounds tested and their purity as supplied by the vendor. Figure S2: Comparison of the co-crystal position of SAH in the catalytic site of DNMT1 (PDB ID: 4WXX) with the predicted binding mode of (A) CSC027694519 and (B) 7936171. Figure S3: Docking poses of glyburide with DNMT1 obtained with the software PLANTS. Figure S4: Microstate network analysis of glyburide.

Author Contributions: Conceptualization, J.L.M.-F.; methodology, K.E.J.-M., F.D.P.-M., N.S.-C., A.P.-C. and D.P.-G.; formal analysis, K.E.J.-M., F.D.P.-M., N.S.-C., A.P.-C., D.P.-G. and J.L.M.-F.; resources, J.L.M.-F. and D.P.-G.; writing—original draft preparation, K.E.J.-M. and J.L.M.-F.; writing—review and editing, all authors; supervision, J.L.M.-F. and D.P.-G.; project administration, J.L.M.-F.; funding acquisition, J.L.M.-F. All authors have read and agreed to the published version of the manuscript.

Funding: This research was funded by the *Consejo Nacional de Ciencia y Tecnología* (CONACyT), Mexico (grant 282785). K.E.J.-M. thanks the support from CONACyT. N.S.-C. and F.D.P.-M. are also thankful to CONACyT for the PhD scholarships no. 335997 and 660465/576637, respectively.

Institutional Review Board Statement: Not applicable.

Informed Consent Statement: Not applicable.

Data Availability Statement: The data presented in this study are available in the main text and the Supplementary Materials.

Acknowledgments: Valuable discussions with Oscar Méndez-Lucio, Jennifer Tamayo, Carlos Velazquez, and Miguel Herrera are highly appreciated.

Conflicts of Interest: The authors declare no conflict of interest.

References

1. Waddington, C.H. The epigenotype, endeavor, 1942, vol. 1 (pg. 18-20) reprinted in. *Int. J. Epidemiol.* **2012**, *41*, 10–13. [CrossRef] [PubMed]
2. Greally, J.M. A user's guide to the ambiguous word 'epigenetics'. *Nat. Rev. Mol. Cell Biol.* **2018**, *19*, 207–208. [CrossRef] [PubMed]
3. Wu, C.; Morris, J.R. Genes, genetics, and epigenetics: A correspondence. *Science* **2001**, *293*, 1103–1105. [CrossRef] [PubMed]
4. Cavalli, G.; Heard, E. Advances in epigenetics link genetics to the environment and disease. *Nature* **2019**, *571*, 489–499. [CrossRef]
5. Ganesan, A.; Arimondo, P.B.; Rots, M.G.; Jeronimo, C.; Berdasco, M. The timeline of epigenetic drug discovery: From reality to dreams. *Clin. Epigenet.* **2019**, *11*, 174. [CrossRef]
6. Sessions, Z.; Sánchez-Cruz, N.; Prieto-Martínez, F.D.; Alves, V.M.; Santos, H.P., Jr.; Muratov, E.; Tropsha, A.; Medina-Franco, J.L. Recent progress on cheminformatics approaches to epigenetic drug discovery. *Drug Discov. Today* **2020**, *25*, 2268–2276. [CrossRef]
7. Lyko, F. The DNA methyltransferase family: A versatile toolkit for epigenetic regulation. *Nat. Rev. Genet.* **2017**, *19*, 81. [CrossRef]
8. Zhang, J.; Yang, C.; Wu, C.; Cui, W.; Wang, L. DNA methyltransferases in cancer: Biology, paradox, aberrations, and targeted therapy. *Cancers* **2020**, *12*, 2123. [CrossRef]
9. Estey, E.H. Epigenetics in clinical practice: The examples of azacitidine and decitabine in myelodysplasia and acute myeloid leukemia. *Leukemia* **2013**, *27*, 1803–1812. [CrossRef]
10. Yu, J.; Xie, T.; Wang, Z.; Wang, X.; Zeng, S.; Kang, Y.; Hou, T. DNA methyltransferases: Emerging targets for the discovery of inhibitors as potent anticancer drugs. *Drug Discov. Today* **2019**, *24*, 2323–2331. [CrossRef]
11. Arguelles, A.O.; Meruvu, S.; Bowman, J.D.; Choudhury, M. Are epigenetic drugs for diabetes and obesity at our door step? *Drug Discovery Today* **2016**, *21*, 499–509. [CrossRef] [PubMed]
12. Teitell, M.; Richardson, B. Dna methylation in the immune system. *Clin. Immunol.* **2003**, *109*, 2–5. [CrossRef]
13. Weng, Y.-L.; An, R.; Shin, J.; Song, H.; Ming, G.-L. DNA modifications and neurological disorders. *Neurotherapeutics* **2013**, *10*, 556–567. [CrossRef] [PubMed]
14. de Lera, A.R.; Ganesan, A. Two-hit wonders: The expanding universe of multitargeting epigenetic agents. *Curr. Opin. Chem. Biol.* **2020**, *57*, 135–154. [CrossRef]
15. Rabal, O.; San José-Enériz, E.; Agirre, X.; Sánchez-Arias, J.A.; Vilas-Zornoza, A.; Ugarte, A.; de Miguel, I.; Miranda, E.; Garate, L.; Fraga, M.; et al. Discovery of reversible DNA methyltransferase and lysine methyltransferase g9a inhibitors with antitumoral in vivo efficacy. *J. Med. Chem.* **2018**, *61*, 6518–6545. [CrossRef]
16. López-López, E.; Rabal, O.; Oyarzabal, J.; Medina-Franco, J.L. Towards the understanding of the activity of g9a inhibitors: An activity landscape and molecular modeling approach. *J. Comp. Aided Mol. Des.* **2020**, *34*, 659–669. [CrossRef]
17. Yuan, Z.; Chen, S.; Gao, C.; Dai, Q.; Zhang, C.; Sun, Q.; Lin, J.-S.; Guo, C.; Chen, Y.; Jiang, Y. Development of a versatile DNMT and HDAC inhibitor C02S modulating multiple cancer hallmarks for breast cancer therapy. *Bioorg. Chem.* **2019**, *87*, 200–208. [CrossRef]
18. Arce, C.; Segura-Pacheco, B.; Perez-Cardenas, E.; Taja-Chayeb, L.; Candelaria, M.; Dueñnas-Gonzalez, A. Hydralazine target: From blood vessels to the epigenome. *J. Transl. Med.* **2006**, *4*, 10. [CrossRef]
19. Kim, H.; Kim, J.; Chie, E.; DaYoung, P.; Kim, I.; Kim, I. DNMT (DNA methyltransferase) inhibitors radiosensitize human cancer cells by suppressing DNA repair activity. *Radiat. Oncol.* **2012**, *7*, 39. [CrossRef]
20. Schcolnik-Cabrera, A.; Domínguez-Gómez, G.; Dueñas-González, A. Comparison of DNA demethylating and histone deacetylase inhibitors hydralazine-valproate versus vorinostat-decitabine incutaneous t-cell lymphoma in HUT78 cells. *Am. J. Blood Res.* **2018**, *8*, 5–16.
21. Singh, N.; Dueñas-González, A.; Lyko, F.; Medina-Franco, J.L. Molecular modeling and dynamics studies of hydralazine with human DNA methyltransferase 1. *ChemMedChem* **2009**, *4*, 792–799. [CrossRef] [PubMed]
22. Kuck, D.; Singh, N.; Lyko, F.; Medina-Franco, J.L. Novel and selective DNA methyltransferase inhibitors: Docking-based virtual screening and experimental evaluation. *Bioorg. Med. Chem.* **2010**, *18*, 822–829. [CrossRef] [PubMed]
23. Kuck, D.; Caulfield, T.; Lyko, F.; Medina-Franco, J.L. Nanaomycin a selectively inhibits DNMT3b and reactivates silenced tumor suppressor genes in human cancer cells. *Mol. Cancer Ther.* **2010**, *9*, 3015–3023. [CrossRef] [PubMed]
24. Yoo, J.; Medina-Franco, J.L. Trimethylaurintricarboxylic acid inhibits human DNA methyltransferase 1: Insights from enzymatic and molecular modeling studies. *J. Mol. Model.* **2012**, *18*, 1583–1589. [CrossRef] [PubMed]
25. Yoo, J.; Kim, J.H.; Robertson, K.D.; Medina-Franco, J.L. Molecular modeling of inhibitors of human DNA methyltransferase with a crystal structure: Discovery of a novel DNMT1 inhibitor. *Adv. Protein Chem. Struct. Biol.* **2012**, *87*, 219–247. [PubMed]
26. Méndez-Lucio, O.; Tran, J.; Medina-Franco, J.L.; Meurice, N.; Muller, M. Towards drug repurposing in epigenetics: Olsalazine as a novel hypomethylating compound active in a cellular context. *ChemMedChem* **2014**, *9*, 560–565. [CrossRef]

27. Aldawsari, F.S.; Aguayo-Ortiz, R.; Kapilashrami, K.; Yoo, J.; Luo, M.; Medina-Franco, J.L.; Velázquez-Martínez, C.A. Resveratrol-salicylate derivatives as selective DNMT3 inhibitors and anticancer agents. *J. Enzyme Inhib. Med. Chem.* **2016**, *31*, 695–703. [CrossRef]
28. Davide, G.; Sandra, A.; Emily, B.; Mattia, C.; Marta, G.; Annalisa, C.; Livio, S.; Gianluca, M.; Chiara, C.; Eli, F.-d.G.; et al. Design and synthesis of N-benzoyl amino acid derivatives as DNA methylation inhibitors. *Chem. Biol. Drug Des.* **2016**, *88*, 664–676.
29. Palomino-Hernandez, O.; Jardinez-Vera, A.; Medina-Franco, J. Progress on the computational development of epigenetic modulators of dna methyltransferases 3A and 3B. *J. Mex. Chem. Soc.* **2017**, *61*, 266–272. [CrossRef]
30. Pechalrieu, D.; Dauzonne, D.; Arimondo, P.B.; Lopez, M. Synthesis of novel 3-halo-3-nitroflavanones and their activities as DNA methyltransferase inhibitors in cancer cells. *Eur. J. Med. Chem.* **2020**, *186*, 111829. [CrossRef]
31. Shao, Z.; Xu, P.; Xu, W.; Li, L.; Liu, S.; Zhang, R.; Liu, Y.-C.; Zhang, C.; Chen, S.; Luo, C. Discovery of novel DNA methyltransferase 3a inhibitors via structure-based virtual screening and biological assays. *Bioorg. Med. Chem. Lett.* **2017**, *27*, 342–346. [CrossRef] [PubMed]
32. Krishna, S.; Shukla, S.; Lakra, A.D.; Meeran, S.M.; Siddiqi, M.I. Identification of potent inhibitors of DNA methyltransferase 1 (DNMT1) through a pharmacophore-based virtual screening approach. *J. Mol. Graph. Model.* **2017**, *75*, 174–188. [CrossRef] [PubMed]
33. Erdmann, A.; Arimondo, P.B.; Guianvarc'h, D. Structure-guided optimization of DNA methyltransferase inhibitors. In *Epi-Informatics*; Medina-Franco, J.L., Ed.; Academic Press: London, UK, 2016; pp. 53–74.
34. Joshi, M.; Rajpathak, S.N.; Narwade, S.C.; Deobagkar, D. Ensemble-based virtual screening and experimental validation of inhibitors targeting a novel site of human DNMT1. *Chem. Biol. Drug Des.* **2016**, *88*, 5–16. [CrossRef] [PubMed]
35. Kabro, A.; Lachance, H.; Marcoux-Archambault, I.; Perrier, V.; Dore, V.; Gros, C.; Masson, V.; Gregoire, J.M.; Ausseil, F.; Cheishvili, D.; et al. Preparation of phenylethylbenzamide derivatives as modulators of dnmt3 activity. *MedChemComm* **2013**, *4*, 1562–1570. [CrossRef]
36. Castellano, S.; Kuck, D.; Viviano, M.; Yoo, J.; López-Vallejo, F.; Conti, P.; Tamborini, L.; Pinto, A.; Medina-Franco, J.L.; Sbardella, G. Synthesis and biochemical evaluation of δ2-isoxazoline derivatives as DNA methyltransferase 1 inhibitors. *J. Med. Chem.* **2011**, *54*, 7663–7677. [CrossRef]
37. Newton, A.S.; Faver, J.C.; Micevic, G.; Muthusamy, V.; Kudalkar, S.N.; Bertoletti, N.; Anderson, K.S.; Bosenberg, M.W.; Jorgensen, W.L. Structure-guided identification of DNMT3b inhibitors. *ACS Med. Chem. Lett.* **2020**, *11*, 971–976. [CrossRef]
38. Naveja, J.J.; Medina-Franco, J.L. Insights from pharmacological similarity of epigenetic targets in epipolypharmacology. *Drug Discov. Today* **2018**, *23*, 141–150. [CrossRef]
39. Medina-Franco, J.L.; López-Vallejo, F.; Kuck, D.; Lyko, F. Natural products as DNA methyltransferase inhibitors: A computer-aided discovery approach. *Mol. Divers.* **2011**, *15*, 293–304. [CrossRef]
40. Saldívar-González, F.I.; Gómez-García, A.; Chávez-Ponce de León, D.E.; Sánchez-Cruz, N.; Ruiz-Rios, J.; Pilón-Jiménez, B.A.; Medina-Franco, J.L. Inhibitors of DNA methyltransferases from natural sources: A computational perspective. *Front. Pharmacol.* **2018**, *9*, 1144. [CrossRef]
41. Akone, S.H.; Ntie-Kang, F.; Stuhldreier, F.; Ewonkem, M.B.; Noah, A.M.; Mouelle, S.E.M.; Müller, R. Natural products impacting DNA methyltransferases and histone deacetylases. *Front. Pharmacol.* **2020**, *11*, 992. [CrossRef]
42. Lee, W.J.; Shim, J.Y.; Zhu, B.T. Mechanisms for the inhibition of DNA methyltransferases by tea catechins and bioflavonoids. *Mol. Pharmacol.* **2005**, *68*, 1018–1030. [CrossRef] [PubMed]
43. Lee, W.J.; Zhu, B.T. Inhibition of DNA methylation by caffeic acid and chlorogenic acid, two common catechol-containing coffee polyphenols. *Carcinogenesis* **2006**, *27*, 269–277. [CrossRef] [PubMed]
44. Martinez-Mayorga, K.; Montes, C.P. The role of nutrition in epigenetics and recent advances of in silico studies. In *Epi-Informatics*; Medina-Franco, J.L., Ed.; Academic Press: London, UK, 2016; pp. 385–398.
45. Prieto-Martínez, F.; Peña-Castillo, A.; Méndez-Lucio, O.; Fernández-de Gortari, E.; Medina-Franco, J.L. Molecular modeling and chemoinformatics to advance the development of modulators of epigenetic targets: A focus on DNA methyltransferases. *Adv. Protein Chem. Struct. Biol.* **2016**, *105*, 1–26. [PubMed]
46. Medina-Franco, J.L.; Méndez-Lucio, O.; Yoo, J.; Dueñas, A. Discovery and development of DNA methyltransferase inhibitors using in silico approaches. *Drug Discov. Today* **2015**, *20*, 569–577. [CrossRef] [PubMed]
47. Yuan, Z.; Sun, Q.; Li, D.; Miao, S.; Chen, S.; Song, L.; Gao, C.; Chen, Y.; Tan, C.; Jiang, Y. Design, synthesis and anticancer potential of NSC-319745 hydroxamic acid derivatives as DNMT and HDAC inhibitors. *Eur. J. Med. Chem.* **2017**, *134*, 281–292. [CrossRef]
48. Erdmann, A.; Halby, L.; Fahy, J.; Arimondo, P.B. Targeting DNA methylation with small molecules: What's next? *J. Med. Chem.* **2014**, *58*, 2569–2583. [CrossRef]
49. Gros, C.; Fleury, L.; Nahoum, V.; Faux, C.; Valente, S.; Labella, D.; Cantagrel, F.; Rilova, E.; Bouhlel, M.A.; David-Cordonnier, M.-H.; et al. New insights on the mechanism of quinoline-based DNA methyltransferase inhibitors. *J. Biol. Chem.* **2015**, *290*, 6293–6302. [CrossRef]
50. Anandakrishnan, R.; Drozdetski, A.; Walker, R.C.; Onufriev, A.V. Speed of conformational change: Comparing explicit and implicit solvent molecular dynamics simulations. *Biophys. J.* **2015**, *108*, 1153–1164. [CrossRef]
51. Röblitz, S.; Weber, M. Fuzzy spectral clustering by PCCA+: Application to Markov state models and data classification. *Adv. Data Anal. Classif.* **2013**, *7*, 147–179. [CrossRef]

52. Podvinec, M.; Lim, S.P.; Schmidt, T.; Scarsi, M.; Wen, D.; Sonntag, L.S.; Sanschagrin, P.; Shenkin, P.S.; Schwede, T. Novel inhibitors of dengue virus methyltransferase: Discovery by in vitro-driven virtual screening on a desktop computer grid. *J. Med. Chem.* **2010**, *53*, 1483–1495. [CrossRef]
53. Guianvarc'h, D.; Arimondo, P.B. Challenges in developing novel DNA methyltransferases inhibitors for cancer therapy. *Fut. Med. Chem.* **2014**, *6*, 1237–1240. [CrossRef] [PubMed]
54. Xu, P.; Hu, G.; Luo, C.; Liang, Z. DNA methyltransferase inhibitors: An updated patent review (2012–2015). *Expert Opin. Ther. Pat.* **2016**, *26*, 1017–1030. [CrossRef] [PubMed]
55. Chen, W.; Seefeldt, T.; Young, A.; Zhang, X.; Guan, X. Design, synthesis, and biological evaluation of n-acetyl-s-(p-chlorophenylcarbamoyl)cysteine and its analogs as a novel class of anticancer agents. *Bioorg. Med. Chem.* **2011**, *19*, 287–294. [CrossRef]
56. Wu, Y.; Liu, H.-B.; Shi, X.-F.; Song, Y. Conventional hypoglycaemic agents and the risk of lung cancer in patients with diabetes: A meta-analysis. *PLoS ONE* **2014**, *9*, e99577. [CrossRef]
57. Prince, H.M.; Bishton, M.J.; Johnstone, R.W. Panobinostat (lbh589): A potent pan-deacetylase inhibitor with promising activity against hematologic and solid tumors. *Future Oncol.* **2009**, *5*, 601–612. [CrossRef] [PubMed]
58. Choi, S.A.; Lee, C.; Kwak, P.A.; Park, C.-K.; Wang, K.-C.; Phi, J.H.; Lee, J.Y.; Chong, S.; Kim, S.-K. Histone deacetylase inhibitor panobinostat potentiates the anti-cancer effects of mesenchymal stem cell-based strail gene therapy against malignant glioma. *Cancer Lett.* **2019**, *442*, 161–169. [CrossRef]
59. Jung, M.; Kim, S.; Lee, J.-K.; Yoon, S.O.; Park, H.S.; Hong, S.W.; Park, W.-S.; Kim, J.E.; Kim, J.; Keam, B.; et al. Clinicopathological and preclinical findings of nut carcinoma: A multicenter study. *Oncologist* **2019**, *24*, e740–e748. [CrossRef] [PubMed]
60. Matsuda, Y.; Yamauchi, T.; Hosono, N.; Uzui, K.; Negoro, E.; Morinaga, K.; Nishi, R.; Yoshida, A.; Kimura, S.; Maekawa, T.; et al. Combination of panobinostat with ponatinib synergistically overcomes imatinib-resistant CML cells. *Cancer Sci.* **2016**, *107*, 1029–1038. [CrossRef] [PubMed]
61. Zopf, S.; Ocker, M.; Neureiter, D.; Alinger, B.; Gahr, S.; Neurath, M.F.; Di Fazio, P. Inhibition of DNA methyltransferase activity and expression by treatment with the pan-deacetylase inhibitor panobinostat in hepatocellular carcinoma cell lines. *BMC Cancer* **2012**, *12*, 386. [CrossRef]
62. Steele, N.; Finn, P.; Brown, R.; Plumb, J.A. Combined inhibition of DNA methylation and histone acetylation enhances gene re-expression and drug sensitivity in vivo. *Br. J. Cancer* **2009**, *100*, 758–763. [CrossRef]
63. Min, H.-Y.; Lee, S.-C.; Woo, J.K.; Jung, H.J.; Park, K.H.; Jeong, H.M.; Hyun, S.Y.; Cho, J.; Lee, W.; Park, J.E.; et al. Essential role of DNA methyltransferase 1–mediated transcription of insulin-like growth factor 2 in resistance to histone deacetylase inhibitors. *Clin. Cancer Res.* **2017**, *23*, 1299. [CrossRef] [PubMed]
64. Morel, D.; Jeffery, D.; Aspeslagh, S.; Almouzni, G.; Postel-Vinay, S. Combining epigenetic drugs with other therapies for solid tumours—Past lessons and future promise. *Nat. Rev.Clin. Oncol.* **2020**, *17*, 91–107. [CrossRef] [PubMed]
65. Rajavelu, A.; Tulyasheva, Z.; Jaiswal, R.; Jeltsch, A.; Kuhnert, N. The inhibition of the mammalian DNA methyltransferase 3a (DNMT3a) by dietary black tea and coffee polyphenols. *BMC Biochem.* **2011**, *12*, 16. [CrossRef] [PubMed]
66. Castillo-Aguilera, O.; Depreux, P.; Halby, L.; Arimondo, P.; Goossens, L. DNA methylation targeting: The DNMT/HMT crosstalk challenge. *Biomolecules* **2017**, *7*, 3. [CrossRef] [PubMed]
67. López-López, E.; Prieto-Martínez, F.D.; Medina-Franco, J.L. Activity landscape and molecular modeling to explore the SAR of dual epigenetic inhibitors: A focus on g9a and DNMT1. *Molecules* **2018**, *23*, 3282. [CrossRef]
68. Prinz, J.H.; Wu, H.; Sarich, M.; Keller, B.; Senne, M.; Held, M.; Chodera, J.D.; Schütte, C.; Noé, F. Markov models of molecular kinetics: Generation and validation. *J. Chem. Phys.* **2011**, *134*, 174105. [CrossRef]
69. López-López, E.; Barrientos-Salcedo, C.; Prieto-Martínez, F.D.; Medina-Franco, J.L. In silico tools to study molecular targets of neglected diseases: Inhibition of TcSir2rp3, an epigenetic enzyme of *Trypanosoma cruzi*. *Adv. Protein Chem. Struct. Biol.* **2020**, *122*, 203–229.
70. Sánchez-Cruz, N.; Medina-Franco, J.L.; Mestres, J.; Barril, X. Extended connectivity interaction features: Improving binding affinity prediction through chemical description. *Bioinformatic* **2020**, in press. [CrossRef]
71. Reaction Biology Corporation. Available online: http://www.reactionbiology.com (accessed on 12 December 2020).
72. Molecular Operating Environment (MOE), Version 2018.08, Chemical Computing Group Inc.: Montreal, QC, Canada. Available online: http://www.chemcomp.com (accessed on 12 December 2020).
73. Berman, H.M.; Westbrook, J.; Feng, Z.; Gilliland, G.; Bhat, T.N.; Weissig, H.; Shindyalov, I.N.; Bourne, P.E. The protein data bank. *Nucl. Acids Res.* **2000**, *28*, 235–242. [CrossRef]
74. Zhang, Z.-M.; Liu, S.; Lin, K.; Luo, Y.; Perry, J.J.; Wang, Y.; Song, J. Crystal structure of human DNA methyltransferase 1. *J. Mol. Biol.* **2015**, *427*, 2520–2531. [CrossRef]
75. Wang, R.; Lai, L.; Wang, S. Further development and validation of empirical scoring functions for structure-based binding affinity prediction. *J. Comp. Aided Mol. Des.* **2002**, *16*, 11–26. [CrossRef] [PubMed]
76. Onufriev, A.; Bashford, D.; Case, D.A. Exploring protein native states and large-scale conformational changes with a modified generalized born model. *Proteins* **2004**, *55*, 383–394. [CrossRef] [PubMed]
77. Korb, O.; Stützle, T.; Exner, T.E. Empirical scoring functions for advanced protein-ligand docking with PLANTS. *J. Chem. Inf. Model.* **2009**, *49*, 84–96. [CrossRef]

78. Ren, X.; Shi, Y.S.; Zhang, Y.; Liu, B.; Zhang, L.H.; Peng, Y.B.; Zeng, R. Novel consensus docking strategy to improve ligand pose prediction. *J. Chem. Inf. Model.* **2018**, *58*, 1662–1668. [CrossRef] [PubMed]
79. Maier, J.A.; Martinez, C.; Kasavajhala, K.; Wickstrom, L.; Hauser, K.E.; Simmerling, C. Ff14sb: Improving the accuracy of protein side chain and backbone parameters from ff99sb. *J. Chem. Theory Comput.* **2015**, *11*, 3696–3713. [CrossRef]
80. Aaqvist, J.; Warshel, A. Free energy relationships in metalloenzyme-catalyzed reactions. Calculations of the effects of metal ion substitutions in staphylococcal nuclease. *J. Am. Chem. Soc.* **1990**, *112*, 2860–2868. [CrossRef]
81. Liao, Q.; Pabis, A.; Strodel, B.; Kamerlin, S.C.L. Extending the nonbonded cationic dummy model to account for ion-induced dipole interactions. *J. Phys. Chem. Lett.* **2017**, *8*, 5408–5414. [CrossRef]
82. Eastman, P.; Swails, J.; Chodera, J.D.; McGibbon, R.T.; Zhao, Y.; Beauchamp, K.A.; Wang, L.P.; Simmonett, A.C.; Harrigan, M.P.; Stern, C.D.; et al. Openmm 7: Rapid development of high performance algorithms for molecular dynamics. *PLoS Comput. Biol.* **2017**, *13*, e1005659. [CrossRef]
83. McGibbon, R.T.; Beauchamp, K.A.; Harrigan, M.P.; Klein, C.; Swails, J.M.; Hernández, C.X.; Schwantes, C.R.; Wang, L.P.; Lane, T.J.; Pande, V.S. Mdtraj: A modern open library for the analysis of molecular dynamics trajectories. *Biophys. J.* **2015**, *109*, 1528–1532. [CrossRef]
84. Hagberg, A.; Schult, D.; Swart, P. Exploring network structure, dynamics, and function using networkx. In *Proceedings of the 7th Python in Science Conference (SciPy 2008)*; Varoquaux, G., Vaught, T., Millman, J., Eds.; SciPy Conference: Pasadena, CA, USA, 2008; pp. 11–15.
85. Swinburne, T.D.; Wales, D.J. Defining, calculating, and converging observables of a kinetic transition network. *J. Chem. Theory Comput.* **2020**, *16*, 2661–2679. [CrossRef]
86. Scherer, M.K.; Trendelkamp-Schroer, B.; Paul, F.; Pérez-Hernández, G.; Hoffmann, M.; Plattner, N.; Wehmeyer, C.; Prinz, J.-H.; Noé, F. Pyemma 2: A software package for estimation, validation, and analysis of markov models. *J. Chem. Theory Comput.* **2015**, *11*, 5525–5542. [CrossRef] [PubMed]
87. Plattner, N.; Noé, F. Protein conformational plasticity and complex ligand-binding kinetics explored by atomistic simulations and Markov models. *Nat. Commun.* **2015**, *6*, 7653. [CrossRef] [PubMed]
88. Husic, B.E.; Pande, V.S. Markov state models: From an art to a science. *J. Am. Chem. Soc.* **2018**, *140*, 2386–2396. [CrossRef] [PubMed]
89. Jurrus, E.; Engel, D.; Star, K.; Monson, K.; Brandi, J.; Felberg, L.E.; Brookes, D.H.; Wilson, L.; Chen, J.; Liles, K.; et al. Improvements to the APBS biomolecular solvation software suite. *Protein Sci.* **2018**, *27*, 112–128. [CrossRef] [PubMed]